Electronic Supplementary Material (ESI) for Soft Matter.

Supporting Information

Structural characterization of monolayer α,ω DH6T-films grown at the liquid-liquid interface

Manuel Johnson,*[a] Tim Hawly,*[a] and Mingjian Wu,[b] Erdmann Spiecker[b], Rainer H. Fink[a]

Fig SI1: Preparation of thin films at the liquid-liquid interface

The preparation method proposed by Hu *et al.* is shown in **Fig. SI1**. Several µl of the organic semiconductor (OSC) solution are dropped onto water forming a floating lens on top of the water surface. The beaker is then covered and cooled to 278 K to reduce the evaporation of the solvent. Mainly driven by intermolecular π-π interactions the molecules will self-assemble, leaving behind a crystalline thin film after complete evaporation of the solvent. The water surface acts as defect-free support during the film formation and the liquid surrounding offers better chance for molecular diffusion and self-organization resulting in a near-equilibrium growth of the organic film.

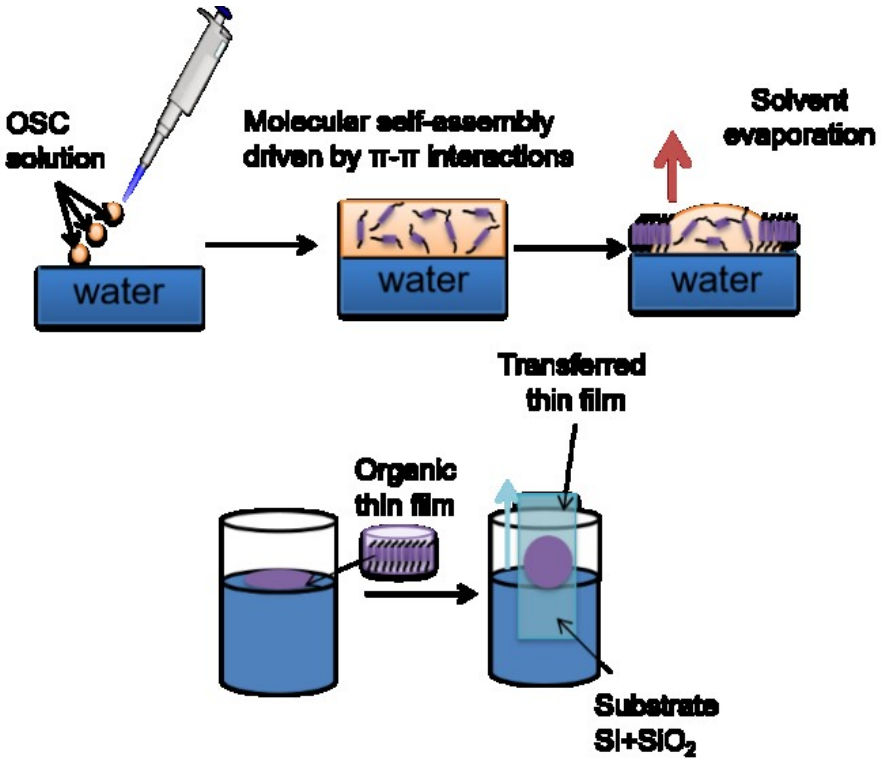

Fig SI1: Schematic representation of the preparation technique.

<u>Fig SI2:</u> Large area electron diffraction of α,ω-DH6T thin films grown at the liquid-liquid interface

Fig. SI 2, left displays a selection area electron diffraction (SAED) pattern of α, ω-DH6T, revealing the single crystalline nature of the thin film. The pattern was recorded using a selection area aperture including an area of 3.5 µm in diameter.

Furthermore, diffraction imaging is applied to evaluate the crystal quality over a larger area. In this technique, the 2-dimensional diffraction pattern at every probed position is recorded while the electron probe was scanned over a 2D sample surface area, thus forming a 4D dataset, also known as 4D-STEM[1,2]. After data acquisition, virtual masks/apertures can be applied to the 4D data to reconstruct real space images (e.g. dark-field images). Here, we applied low-mag STEM mode and set the convergence angle to ~0.2 mrad to access sample area as large as 80 µm x 80 µm, more than an order of magnitude larger than typical SAED can cover. **Fig. SI2, right** shows an evaluated dataset. The dark field image shown in the center is calculated using {020} reflection covers the entire 80 µm x 80 µm area, revealing single crystalline nature of the monolayer over this size. The cracks form during the drying process after the thin film was transferred to the TEM grid. Several underlying raw diffraction patterns at different positions are extracted and shown as insets to the sides of **Fig. SI2, right**. No rotation of the diffraction pattern can be found across the whole image, confirming the long-range crystalline order and absence of grain boundaries.

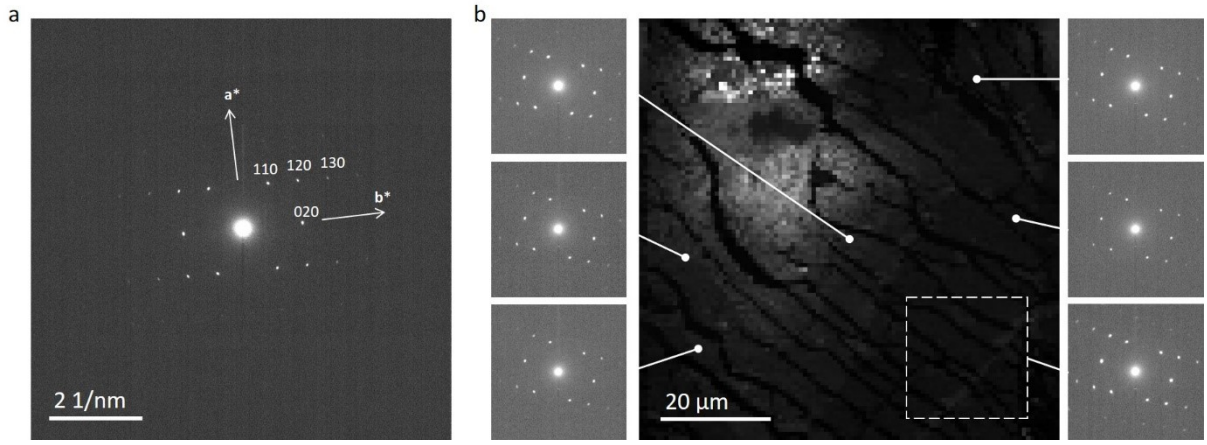

Fig SI2: (left) SAED of α, ω DH6T using an aperture include a circular region of 3.5 µm diameter. (right) Virtual dark field image reconstructed from a diffraction imaging (i.e., 4D dataset) using {020} reflection. 5 underlying raw diffraction patterns extracted from the dotted positions are show as insets; a sum diffraction pattern from a 20x20 µm region is show to the lower right inset. Single crystalline nature of the liquid-liquid prepared α, ω DH6T is confirmed over an area as large as 80x80 µm. The cracks in the dark field image are due to the dying process after the thin have transferred to the TEM grid.

<u>Fig SI3:</u> AFM image of a α,ω-DH6T multilayer area grown at the liquid-liquid interface

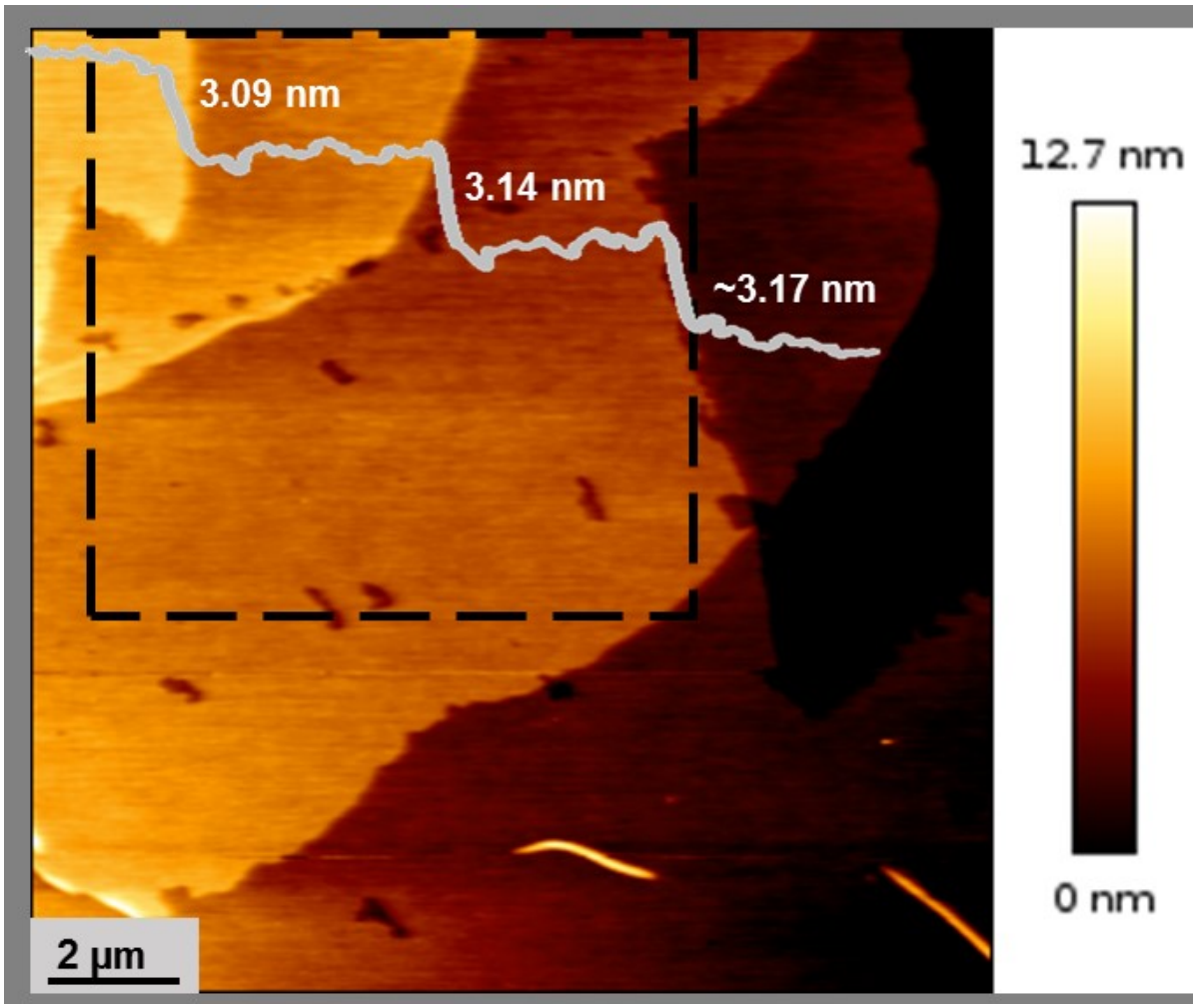

Fig SI3: AFM image of a multilayer area of a solution-processed sample using 50 µl of saturated α,ω-DH6T/Toluene solution with extracted height profiles.

<u>Fig SI4</u>: NEXAFS spectra of vacuum and solution processed α,ω-DH6T samples recorded for different photon incidence angles

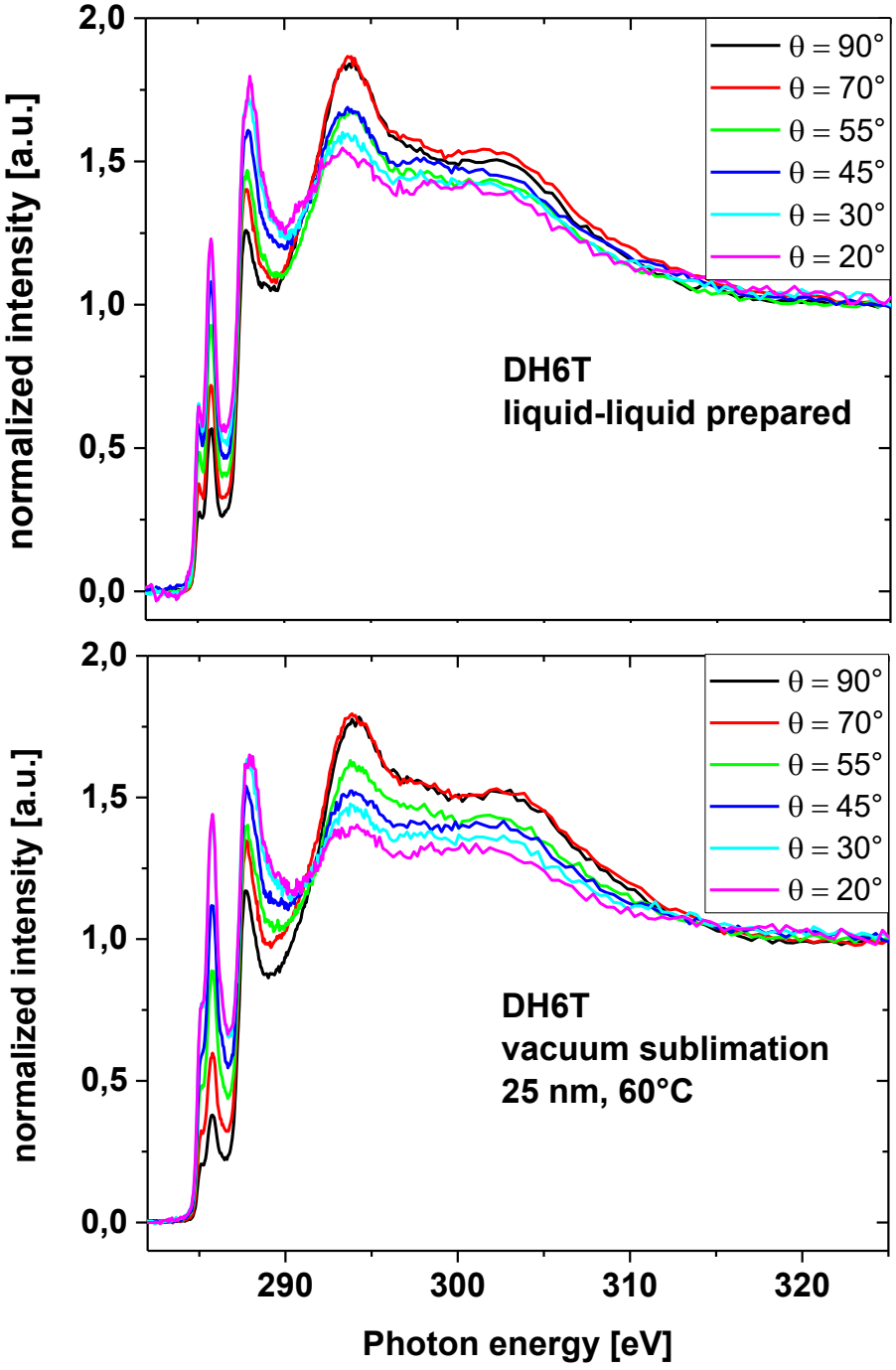

Fig SI4: Polarization dependence of the NEXAFS spectra obtained from α,ω-DH6t thin film. (top) Solution processed (bottom) vacuum sublimated (25 nm at 60°C substrate temperature).

Fig SI5: Fitted NEXAFS spectra of solution processed DH6T thin film

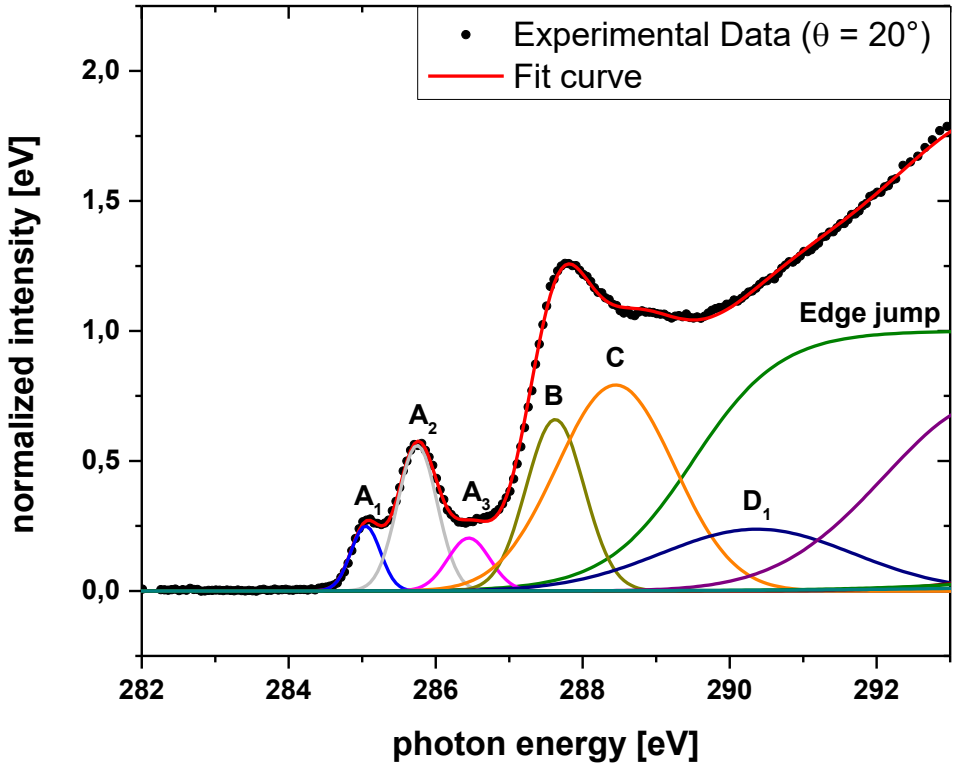

Fig SI5: π-region of the C1s NEXAFS spectra of a solution processed α,ω-DH6T thin film recorded at a photon incidence angle of 20°. The experimental spectrum (black dots) is normalized to the C1s continuum at 320 eV. The overall fit is depicted as red line; the individual fitted peaks are displayed with different colors.

With reference to different thiophene derivatives[4-6] we assigned the peaks in the C1s NEXAFS absorption as shown in Table 1.

Table 1: Peak assignment in the C1s NEXAFS spectra of α,ω -DH6T shown in **Fig S5**.

Peak	Energy [eV]	Assignment	Peak	Energy [eV]	Assignment
A_1	285.05	$\pi^*_{C=C}$	**D_1**	290.37	σ^*_{C-C}
A_2	285.75	$\pi^*_{C=C}$	**D_2**	293.58	σ^*_{C-C}
A_3	286.45	$\pi^*_{C=C}$	**D_3**	296.77	σ^*_{C-C}
B	287.63	$\pi^*_{C=C} + \sigma^*_{C-S}$	**D_4**	301.51	σ^*_{C-C}
C	288.50	σ^*_{C-H}	**D_5**	306.17	σ^*_{C-C}

Section 3: Supplementary References

1. O. Panova, C. Ophus, C. J. Takacs, K. C. Bustillo, L. Balhorn, A. Salleo, N. Balsara and A. M. Minor, *Nature materials*, 2019, **18**, 860-865.
2. C. Ophus, *Microsc. Microanal.*, 2019, **25**, 563-582.
3. M. Waldrip, O. D. Jurchescu, D. J. Gundlach and E. G. Bittle, *Adv. Funct. Mater.*, 2020, **30**, 1904576.
4. G. Tourillon, C. Mahatsekake, C. Andrieu, G. Williams, R. Garrett and W. Braun, *Surf. Sci.*, 1988, **201**, 171-184.
5. P. Väterlein, M. Schmelzer, J. Taborski, T. Krause, F. Viczian, M. Bäßler, R. Fink, E. Umbach and W. Wurth, *Surf. Sci.*, 2000, **452**, 20-32.
6. E. M. Mannebach, J. W. Spalenka, P. S. Johnson, Z. Cai, F. Himpsel and P. G. Evans, *Adv. Funct. Mater.*, 2013, **23**, 554-564.